Available online at www.garmian.edu.krd

Passer Journal

Passer 7 (Issue 1) (2025) 17-28

http://passer.garmian.edu.krd/

Groundwater Risk Intensity Map through Modified DRASTIC Model in the Rania Basin, Kurdistan Region of Iraq

Ata Omer Salih[1], Diary Ali Al-Manmi[2*]

[1]*Department of General Science, College of Education, Charmo University, Chamchamal, Iraq*
[2]*Department of Petroleum and Energy Engineering, Technical College of Engineering (TCE), Sulaimani Polytechnic University, Sulaymaniyah, Iraq*

Received 9 February 2024; revised 8 September 2024;
accepted 2 November 2024; available online 10 December 2024

DOI: 10.24271/PSR.2024.442571.1492

ABSTRACT

Protecting groundwater as the most effective tool in managing water resources has recently drawn the attention it deserves. This project attempts to prepare groundwater's risk intensity index map by combining hazard and intrinsic vulnerability maps. The place of concern is the basin of Rania, located in Iraq's Kurdistan region. The very low and low vulnerability index covered (31.7 %) and (42.5 %) of the basin, while medium and high covered (24 %) and (1.7 %). Hazard maps of the studied basin helped to identify around 17 hazard sources of point, line, and polygon types. The classified hazard map and the lineament-DRASTIC index map were then combined by the European approach technique (COST Action 620) to create a Risk Intensity Index (RII) map, based on which the region was divided into five classes. The majority revealed no, very low, or low-risk levels, whereas high and moderate risk levels only covered a small portion of the studied area. However, the most considerable portion (51.5%) is classed as low risk followed by (31.9%) as moderate risk. In comparison, the risk in 5.6% of the area is deficient, leaving only (10.8%) for high and (0.2%) for the very high categories. All assessment results were calibrated using measured Nitrate concentration. Different vulnerability zones produced by both standard and modified DRASTIC models reflected a progressive increase in Nitrate level.

Keywords: Hazard map, Kurdistan, Lineament-modified DRASTIC model, Risk assessment.

1 Introduction

Groundwater is a vital natural resource that sustains ecosystems and provides drinking water to millions of people globally. Today, groundwater pollution has become a critical concern for communities worldwide. The combination of rapid population growth in developing nations and the impacts of climate change places additional pressure on water supplies, making groundwater reservoirs an essential resource for mitigating these challenges [1,2,3,4]. Iraq, in particular, is currently experiencing severe water shortages, with projections indicating that this scarcity will worsen significantly over the next thirty years [5].

While groundwater is a crucial water source, it also poses significant health risks if contaminated, primarily due to the difficulties associated with its remediation [6]. Preventing contamination through vulnerability mapping and risk assessments is a more practical and cost-effective strategy to preserve the quality of this essential resource. Once groundwater is contaminated, remediation is exceedingly challenging due to its subterranean nature. If the intrinsic properties of the system are inadequate to protect groundwater from surface pollutants, its vulnerability will increase. Consequently, vulnerability assessments are undertaken by numerous governmental and non-governmental organisations across many countries as integral components of their planning, policy formulation, and decision-making processes [7]. The demarcation of pollution susceptibility zones is a crucial measure that must be undertaken to safeguard and efficiently control aquifers [8]. In a study by [9], the groundwater pollution risk is defined as the likelihood that the groundwater within an aquifer will reach an unacceptable level of contamination due to activities occurring on the land surface above it. This approach involves assessing the interaction between pollutant concentrations underground and the vulnerability of the aquifer at specific sites, a process known as "intensity assessment of risk."

The DRASTIC model (Depth to Water, Recharge, Aquifer Media, Soil, Topography, Impact of Vadose Zone, and Conductivity) has been extensively used for assessing groundwater vulnerability since its development by the United States Environmental Protection Agency (EPA) in the 1980s. The model evaluates aquifer vulnerability based on seven parameters. However, it has been criticised for not adequately considering geological characteristics that are crucial in determining

* Corresponding author
E-mail address diary.amin@spu.edu.iq (Instructor).
Peer-reviewed under the responsibility of the University of Garmian.

groundwater vulnerability. Consequently, various modifications and adjustments have been proposed and tested, involving the addition, removal, or alteration of one or more parameters.

In recent years, researchers have emphasised the importance of geological lineaments in influencing groundwater flow and contaminant transport. Lineaments, which include faults, fractures, and joints, significantly affect subsurface water movement and are highly valued by hydrogeologists as they establish pathways for subsurface water flow [5]. To overcome the limitations of the traditional DRASTIC model, numerous studies have suggested incorporating lineament data to enhance the accuracy of groundwater vulnerability assessments. One notable study by [10] examined the Lineament-modified DRASTIC approach in the Ponnaiyar River Basin in India. By incorporating lineament data into the DRASTIC model, the researchers demonstrated that the modified model produced more precise groundwater vulnerability maps. They found that lineaments act as preferential pathways for groundwater flow and contaminant migration, making them essential considerations in risk assessments.

Another study by [11] investigated the application of the Lineament-modified DRASTIC model in a Mediterranean coastal area. The research revealed that the traditional DRASTIC model underestimated aquifer vulnerability due to its failure to account for geological lineaments. By including these features, the study accurately identified areas at higher risk of contamination.

Furthermore, the use of remote sensing and geographic information systems (GIS) has enhanced the effectiveness of the Lineament-modified DRASTIC model. A study by [12] utilised GIS and satellite imagery to identify lineaments and integrate them into the DRASTIC model for groundwater vulnerability assessment in southwestern Nigeria. Their results emphasised the importance of incorporating spatial data to improve the accuracy of risk intensity maps.

Despite these advancements, it is crucial to recognise that integrating lineaments into the DRASTIC model can introduce complexity and data requirements. Therefore, the success of the Lineament-modified DRASTIC model largely depends on the availability of reliable geological data and advanced GIS techniques. Researchers continue to explore ways to simplify this process while maintaining its effectiveness. Additionally, GIS technologies enable the generation of vulnerability and risk maps that are easy to update with changes in development, allowing for the regular inclusion of new data.

Extensive research has been devoted to finding the most accurate, time- and cost-effective methods for assessing groundwater pollution risk, thereby guiding authorities to take necessary steps to prevent or minimise contamination. For example, [13] utilised remote sensing tools to assess groundwater pollution risk. [14] employed the overly index-based PI model to calculate intrinsic vulnerability, combining it with hazard maps to assess groundwater pollution risk intensity in karstic aquifers in Ramallah, Palestine. [15] produced a Pollution Risk Intensity (PRI) map for groundwater in Sulaimani City, Kurdistan, Iraq, by integrating seven factors: Depth to water table (D), Distance to pollutant sources (Ds), Lineament density (Ln), Slope degree (Sr), Soil type (S), Aquifer recharge rates (R), and Lithology of the unsaturated zone (L). [16] combined intrinsic vulnerability, measured through the pesticide-DRASTIC model, with hazard maps to develop a risk intensity map of the Basara basin in the Iraqi Kurdistan region.

This paper aims to create a risk intensity map of groundwater in the Rania basin by combining intrinsic vulnerability and hazard maps, following the European COST Action 620 approach. To improve the accuracy of the assessment, this study modifies the standard DRASTIC model by integrating a lineament density index and calibrating the modified model using measured nitrate levels. The Lineament-modified DRASTIC model, which incorporates geological features such as faults and fractures, offers a more site-specific and realistic evaluation of intrinsic groundwater vulnerability. This approach, in turn, provides a more accurate assessment when incorporated into the risk intensity index. The study's findings will contribute to a more precise risk intensity index and provide valuable insights for improving groundwater management and policy-making.

2 Materials and methods

2.1 Study area

The Rania Basin, covering an area of 1,269.3 km², is located in the Kurdistan Region of Iraq, in the northeastern part of the country (Fig. 1). The basin encompasses the Rania district as well as the sub-districts of Chwarqurna, Hajiawa, Betwata, Hiran, and Nazaneen, along with approximately 200 villages. The Rania district is situated just 10 km from Dokan Lake and 131 km north of Sulaimani city, within the coordinates of 36°05'15" to 36°28'13" latitude and 44°25'38" to 44°58'51" longitude. The basin is predominantly mountainous, with elevations reaching up to 2,400 meters above sea level (m.a.s.l.), while the southern parts feature less undulated plains, with elevations as low as 500 m.a.s.l.

2.2 Geological setting

The Rania basin is situated in the Sulaimaniya-Zakho subzone of the high-folded zone, and the area's structure has strong orogeny-induced raised units that are pretty complicated despite being relatively homogeneous [17]. The crests of the anticlines are composed of formations from Jurassic to early Cretaceous. In contrast, the synclines and flanks are formed by late Cretaceous and, more infrequently, Paleogene beds (Fig. 2). The anticlines of Handren, Pelawan, Rania, and Karookh are the prominent structures of the basin [17].

Quaternary deposit in the area comprises Flood Plain, River Terraces, and Alluvial Fans. Conglomerate, clay, loam, silt, and weathered by-products of the formations mentioned above are the main components of these deposits [18]. Along the sides of the structures, slope sediments have accumulated, and the synclines are filled with gravel and clay. Rania and Chwarqurrna alluvial fans are formed by streams that originate from anticlines. A

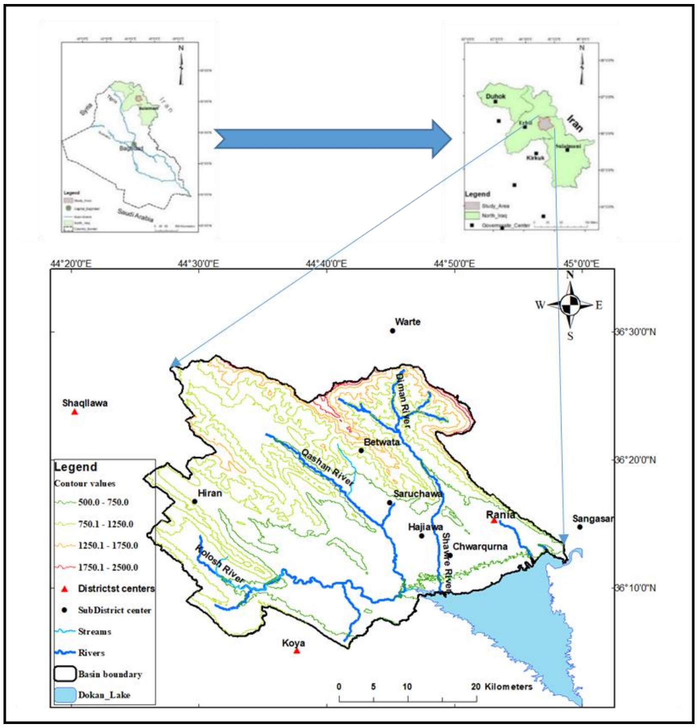

Figure 1: Location of the studied basin.

buildup of frequently shoddy-cemented rocks, gravel, sand, and clays can be found along the waterways. Run-off sand, silt, and clay cover the flat areas between anticlines. Floodplain sediments fill previously developed valleys and contribute to the basin's good-quality aquifers. Quaternary sediments have a thickness that spans from 10 meters to 150 meters in the west and south of the basin.

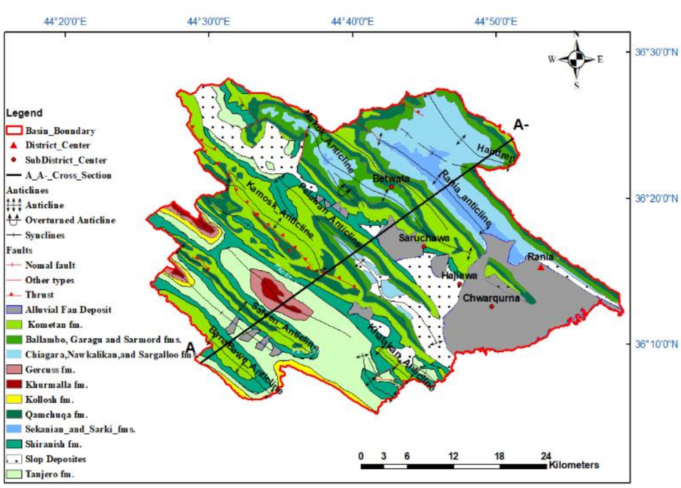

Figure 2: Geological map of the studied basin, modified from[19].

2.3 Hydrogeology

Rania is a part of the lower Zab basin. There is potential for medium- to large-scale irrigation projects in the basin's groundwater resources [17]. Streams, wells, and springs are the area's primary potable water source. Qashan and Diman (Shawre) are the two main rivers that start from the north of the basin and continue their flow downward until they ultimately empty into Dokan Lake. The basin is characterised by the presence of karstic and karstic fissured aquifers in addition to the highly productive Quaternary Sediments that consist of gravel, marl, sand, and silt as shown in (Fig. 3). Cretaceous rock layers of Tanjero, Shiranish, and Qamchuqa formations underlay Quaternary sediments. Shiranish and Qamchuqa formations in the area are also considered promising aquifers.

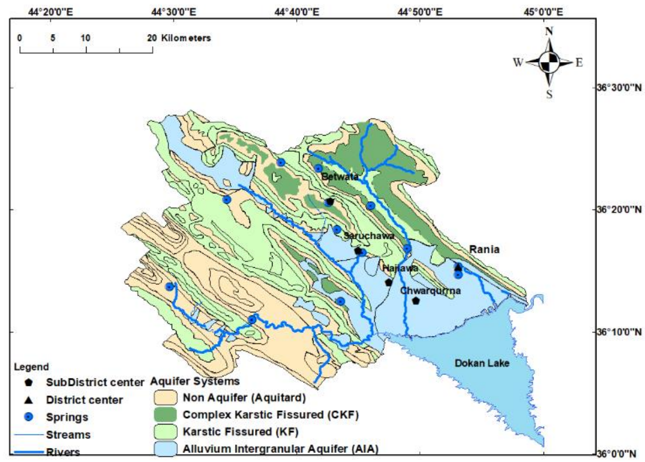

Figure 3: Rania Basin's hydrogeological map.

The principal aquifer in the area is believed to consist of Quaternary deposits. Several systems from various ages, including Jurassic, Quaternary, Late Cretaceous, and Early-late Cretaceous exist in the basin and can be tapped for groundwater as presented in Table 1.

2.4 Work Procedure

The main outline of this research's procedure is focused on a few prominent steps, including:

1. Developing intrinsic vulnerability maps using the standard DRASTIC model with its seven original parameters, as well as a modified model incorporating the lineament density index. The process employs Geographic Information Systems (GIS: ArcMap 10.5) to create the necessary shapefiles.

2. Calibrating pollution assessments using nitrate (NO_3^-) concentration data from 60 water samples collected during wet and dry seasons.

3. Identifying anthropogenic hazard sources to produce both unclassified and classified hazard maps.

4. Constructing the risk intensity map through the combination of the classified hazard and intrinsic vulnerability maps according to [20].

Table 1: Main aquifers in the studied basin.

Aquifer names	Geological formations	Aquifer Types	Lithology	Thickness (m)
Lower Jurassic aquifer	Sarki and Sekanian	Karstic Fissured	Limestone, cherty shale and dark dolomite	300
Upper Jurassic aquifer	Chiagara, Naokalikan, Barsarin and Sargallu	Complex Karstic Fissured	Dolomite, limestone, marl, and organic matter-rich limestone	385
Bekhma Aquifer	Bekhma, Kometan and Qamchuqa	Karstic Fissured	Limestone and dolomite	450
Quaternary Aquifer	Alluvial Fans and Slope Deposits	Intergranular	Gravel, sand, silt and clay	100
Aquitards	Shiranish, Tanjero, Kollosh, Khurmalla and Gercus		Well-bedded limestone, blue marl, siltstone, sandstone and greyish marl	350
Aquiclude	Balambo and Sarmord		Marl, Marley limestone and dolomite	680

2.4.1 Intrinsic Vulnerability Mapping

Generic and modified DRASTIC models have been attempted to assess the basin's intrinsic vulnerability. The model's name is composed of abbreviations from seven factors, each with a particular rate and weight (Table 2). The rates range from one to ten, reflecting the strength of each parameter's impact on groundwater vulnerability. A weight of five represents the most significant factor, while a weight of one represents the least influential factor [20].

Table 2: Ratings and weighting for the generic DRASTIC model based on [21] and modified DRASTIC based on [22].

Parameters	Generic DRASTIC		Modified DRASTIC	
	Rate	Weight	Rate	Weight
Depth to Water Table	1 – 10	5	1 – 10	5
Net Recharge	1 – 9	4	1 – 9	4
Aquifer Media	2 – 10	3	2 – 10	3
Soil Media	1 – 10	2	1 – 10	2
Topography	1 – 10	1	1 – 10	1
Impact of Vadose Zone	1 – 10	5	1 – 10	5
Hydraulic Conductivity	1 – 10	3	1 – 10	3
Lineament Density	-----------	----------	1 - 5	5

The model's index is found according to Eq. (1) as shown below:

$$D = V = \sum_{i=1}^{7}(Wi\ X\ Ri) \quad (1)$$

Whereas; V is the vulnerability value, Wi is the weight of each parameter, and Ri is their rates. The vulnerability index and all its parameters can also be represented linearly in the equation (Eq. 2) below:

$$DI = DwDr + RwRr + AwAr + SwSr + TwTr + IwIr + CwCr \quad (2)$$

D is the distance to water level, R is net recharge, A is the aquifer media, S is the soil media, T is topography, I is the vadose zone's impact and C is hydraulic conductivity.

The Delphi method, which leverages the researcher's field-based expertise and academic insight, was adopted to assign the rates and weights for each parameter.

The measured depth to the water table in 386 wells across the studied basin ranged from 2.5 m (the shallowest) to 104 m (the deepest). Nine depth classes—<4.5 m, 4.5–7.5 m, 7.5–10 m, 10–12.5 m, 12.5–15 m, 15–19 m, 19–23 m, 23–30 m, and >30 m—were assigned rates from 1 to 9, respectively, to construct the D map (Fig. 4a).

The net recharge (R_map) was drawn after the recharge percentages were categorised based on the rates from [21] as shown in Fig.4b.

The four units of Quaternary Intergranular Aquifer (AIA), Karstic Fissured (KF), Complex Karstic Fissured (CKF), and Aquitards have been regrouped and four different rates of (6, 8, 9 and 3) were assigned to them respectively to form A_map (Fig. 4c).

The soil media parameter (S-map) as shown in Fig. 4d was constructed using rating values of 4, 7, 9 and 10 for the four different soil types (silty loamy to clayey, silty clay to clayey, excessively well-drained and thin or absent soil) respectively according to the standard rates recommended by [21].

The topographic map (T_Map) was constructed using a 30m pixel-sized digital elevation model (DEM) of the studied basin in a way that mountainous areas with very steep slopes (>40o) are given the lowest rate of 2 while the shallower area in the south with a very gentle slope (<5o) is assigned the highest rate of 9. The other parts with steep slopes (20o-40o), moderate slopes (10o-20o) and gentle slopes (5o-10o) are given the rates of 4, 6 and 8 (Fig. 4e).

To construct the map of the vadose zone's impact (I_map), as shown in Fig. 4f, five regions were identified, and assigned specific values (3, 4, 5, 6, and 8) based on the standard rates [21].

The rate value of 1 (very low) was assigned to aquifers with the lowest hydraulic conductivity or less than 4m/day, and a rate of 2(low) was given to aquifers with hydraulic conductivity higher than 4m/day (Fig.4g).

2.4.2 Modification with lineament density

The lineament factor is added to the generic model to give it a more accurate representation of groundwater vulnerability. Earlier research has shown a strong relation between lineament and groundwater occurrence, flow, and production [23].

According to [22], the influence of the lineament index can easily be noticed in the groundwater vulnerability assessments when it is incorporated into the generic DRASTIC model (Eq. 3).

$$DL(i) = Di + Li \quad (3)$$

DL (i): Lineament-modified Index; *Di*: Standard Index, *Li*: index of lineament. The many layers of data were processed and represented using Arc GIS 10.5 software in both Generic and modified DRASTIC models. The Rania basin map of lineament distribution was created using pictures from the Landsat 8 Thematic Mapper Plus on November 5, 2020, with a cell size of 30 x 30 meters and the grayscale Operational Land Imager (OLI) spectral band. The lineament distribution over the basin was retrieved using the PCI Geomatica 2017 SP1 software (Fig.5a).

The lineament density maps with ranges and ratings (Fig.5b and Fig.5c) were generated by spatial analysis tool in ArcMap GIS 10.5 using values from Table 3. The likelihood of transferring a pollutant into groundwater increases with the severity of lineament features [18].

Table 3: Rates and weight of lineament index [22].

Range of lineament density	**Rates**
0.2 - 1.1	1
1.2 - 1.3	2
1.4 - 1.5	3
1.5 - 1.8	4
1.9 - 2.0	5
2.1 - 2.2	6
2.3 - 2.4	7
2.5 - 2.6	8
2.7 - 2.8	9
2.9 - 4.0	10
Weight = 5	

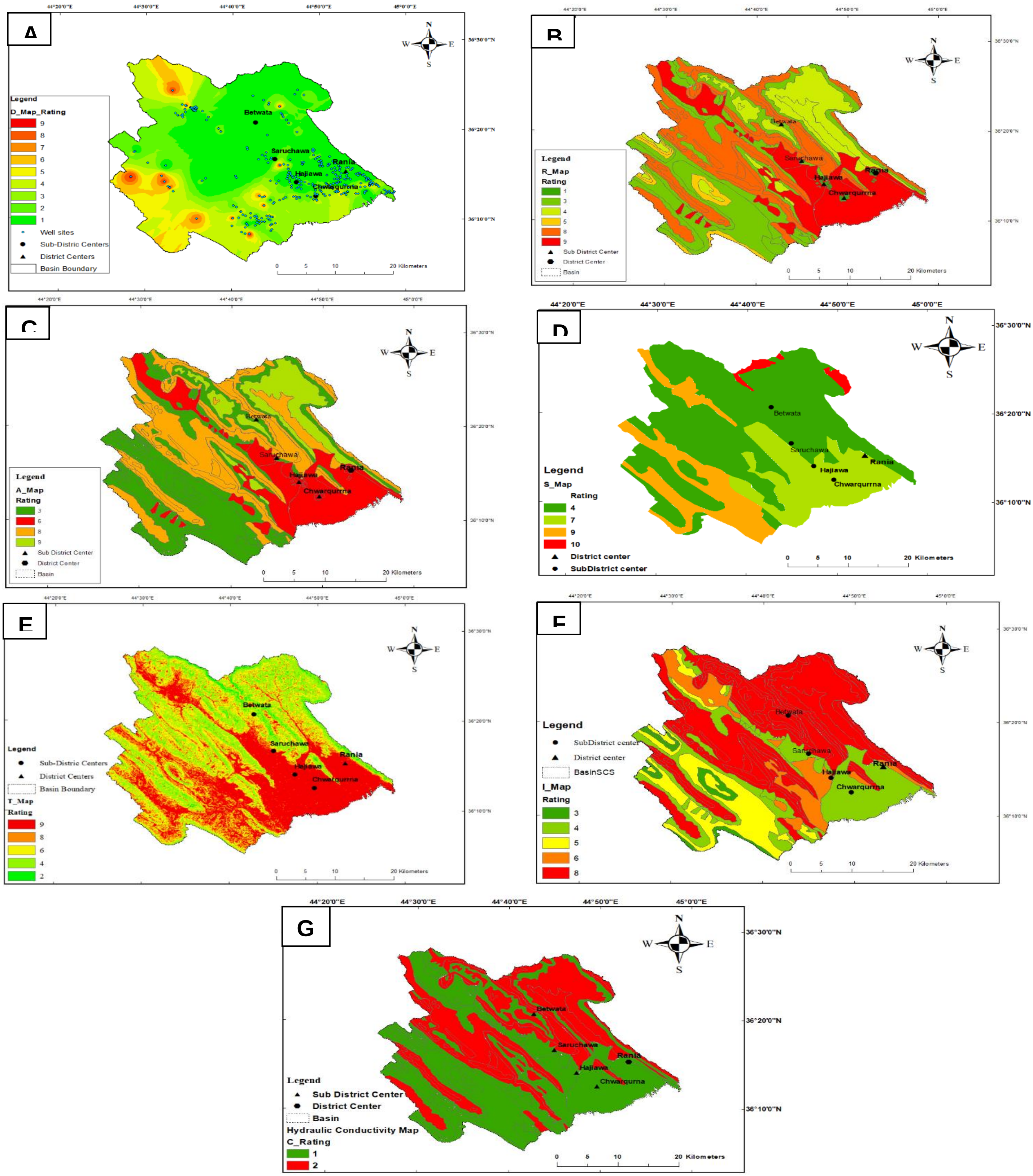

Figure 4: DRASTIC parameter maps: a: depth to groundwater, b: net recharge, c: aquifer media, d: soil media, e: topography, f: impact of vadose zone and g: hydraulic conductivity.

The lineament density was assigned the highest weight coefficient of 5 due to its significant influence [22], and the lineament index map was created by multiplying the rated lineament map by the specified weight using the map algebra tool in ArcMap 10.5 (Fig. 5d).

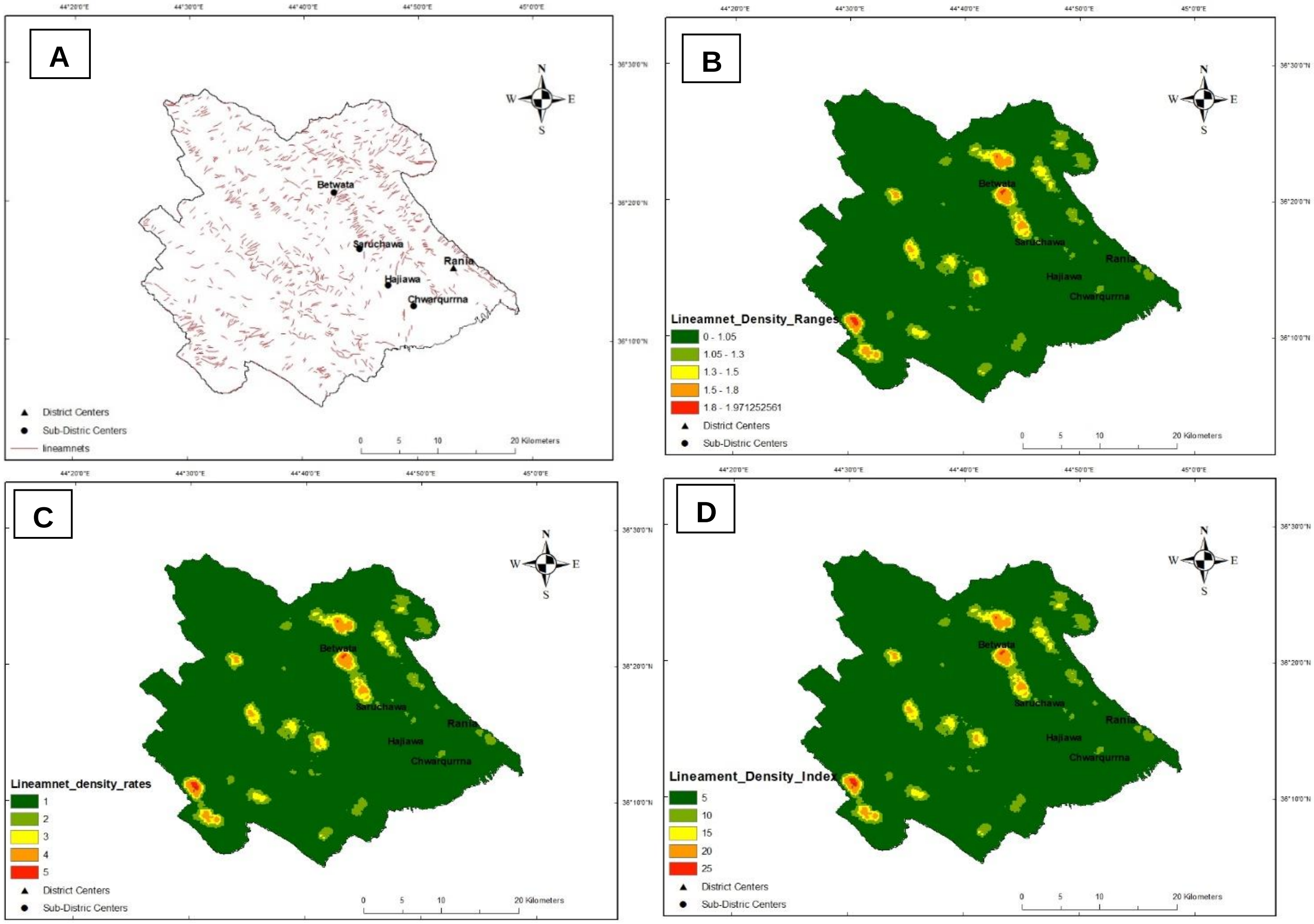

Figure 5: a. Lineament distribution map, b. Lineament density ranges map. c. Lineament density rating map. d. Lineament density index map adopted from [18].

2.4.3 Calibration with Nitrate

The nitrate (NO_3^-) level was used as a reality check for generic and modified phases of the DRASTIC model. Nitrate comes from the nitrogen cycle rather than dissolving minerals, which is how it enters the water supply. Consequently, it might be utilised as a sign of water contamination [23]. Nitrate could also play a vital role in recognising the changes and evolution in groundwater quality [25]. A map of the basin's nitrate distribution was created through the findings of the actual nitrate concentration in groundwater samples collected from 17 water wells in both wet and dry seasons, and compared with the vulnerability maps. Sampling was carried out between October 2018 and May 2019 to illustrate potential fluctuations in nitrate concentration between dry and wet seasons.

2.4.4 Hazard assessment

1. Inventory of hazards and definition

Any potential source of pollution caused by human intervention to the land surface can be defined as a hazard, and any consideration of the probable grade of harmfulness for each kind of hazard is defined as hazard assessment. Hazard level is identified through harmfulness and the amount of unsafe material that could be released by a pollution event [16]. Three levels are suggested by COST Action 620's hazard inventory for choosing the weighting factor. Thus, according to [20] and based on land use, hazards at level one are grouped into three main classes: 1) Industrial activities, 2) Livestock and agriculture, and 3) Infrastructural development (Table 4).

2. Requirements of Hazard Data

When determining the probable degree of harmfulness for every found hazard, knowledge of certain factors is essential. The aspects include the nature of the activity, the type of hazardous materials, the potential quantity of by-products that could enter the system, as well as the age and condition of installations and plants. The collected data are then organised under the headings of determining the activity's nature, localisation of the activity using topographic coordinates, and characterising and measuring the output of solid and liquid waste.

3. Ranking, reduction, and weighting factors

Weights determine the level of hazardousness, while the hazard Index is also slightly influenced by ranking and reduction factors [20]. Inputs of (*H*, *Qn*, and *Rf*) into the columns of attributes were needed to obtain the Hazard Index (HI), as shown in Table 4. To determine the degree of harmfulness of any type of hazard, the hazard index (HI) is calculated using Eq. (4) as described in [13].

$$HI = H * Qn * Rf \tag{4}$$

Where *H* is the weighting value of each hazard, *Qn* is the ranking factor (0.8 to 1.2), and *Rf* is the reduction factor (0 to 1).

Agricultural and urban areas were assessed for the current study based on their size and population.

The industrial sites were assessed based on their activities, including chemical factories, rubber and tire production, food industries, and stockpiles of raw materials and chemicals. These sites were then assigned rankings and reduction factors of 1, 0.5, and 0.55, respectively (Table 4).

Hazards with a high level of harm are given a higher value, such as urban areas with no sewer systems (weighting factor = 70), and hazards with a low level of harm are given a lower value, such as an allotment garden (weighting factor = 15). Accordingly, *Rf* for the study area ranged from (0.5 to 1.0). The harmfulness of the open silage (field), roads, car parking area, Open stadiums, and transformer stations may be lowered due to the lack of a leading pollution source; therefore, a value of (0.8) for *Qn* and (0.5 to 1) for *Rf* was applied.

2.4.5 Hazard Map Production

Urbanisation areas, industrial estates, and agricultural activities are the main features of the studied basin. LULC map, satellite imagery, and walkover surveys were all used to deliver a graphical interpretation of hazard data and define them spatially. ArcMap GIS was chosen to map and colour code different hazards, depicting the degree of their potential harmfulness based on the hazard index Table 4. Such processes included unclassified information, (geographical information) and classified information, based on a hazard index calculation [17].

2.4.6 Risk assessment

Identification of current or possible hazards, as well as exposed groundwater contamination channels, are prominent steps in the risk assessment process. This is done while taking into account the likelihood and severity of potential impacts and groundwater's intrinsic vulnerability [26]. However, this kind of assessment, as explained by [20, 27], is called a "risk intensity map" and computed via the Risk Intensity Index (RII) using (Eq. 5).

$$RII = \frac{1}{HI} \times \pi \tag{5}$$

In a way, *RII is* the risk intensity index, *HI* is the hazard index, and π *is* the intrinsic vulnerability index.

Table 4: Hazard types, H, Qn, Rf, HI and HIC values in the studied basin, modified from [20].

Hazard types	H	Q_n	R_f	HI	HIC	Feature type
Urbanization (leaking sewer pipes and sewer systems)	35	1	0.55	19	1	Polygon
		1	0.6	21		
		1	0.75	26	2	
Urbanization without sewer systems	70	1	0.5	35	2	Polygon
		1	0.6	42		
Storage tank above ground	50	1	0.5	25	2	Polygon
Storage tank underground	55	1	0.55	30	2	
Gasoline station	60	1	0.6	36	2	
Road, unsecured	40	0.8	0.5	16	1	Line
		0.8	0.55	18	1	
		0.8	0.6	19	1	
Road Haulier depot	35	0.8	0.5	14	1	Polygon
Car parking area	35	0.8	0.5	14	1	Point
Tourist urbanization	30	0.8	0.7	17	1	Polygon
		0.8	0.75	18		
Open sport stadium	25	0.8	0.5	10	1	Point
Graveyard	25	0.8	0.8	16	1	Polygon
Transformer station	30	0.8	0.5	12	1	Point
Factories and industrial estates	30	0.8	0.7	17	1	Polygon
Open silage (field)	25	0.8	0.5	10	1	Polygon
Intensive agricultural area (with high demand for fertilizers and pesticides)	30	1	0.8	24	1	Polygon
		1	0.9	27	2	
Allotment garden	15	0.8	0.5	6	1	Point
		0.8	1	12		
Greenhouse	20	0.8	0.8	13	1	

3 Results and Discussions

3.1 Vulnerability classes

The lineament-modified classes show a discernible difference in terms of the area they each represent when compared to classes derived by the standard DRASTIC model. Very low and low vulnerability classes lose 5.3 and 6.5% of the area they cover correspondingly, in comparison, medium and high vulnerability classes gain an extra 10.33 and 1.4 % increase in their coverage Table 5. This change is because of the introduction of lineament features in the index calculation.

Table 5: Covered area and Nitrate (NO3-) concentration for generic and modified DRASTIC vulnerability classes in the studied basin.

Standard DRASTIC Classes	Covered area (Km^2)	Median value of Nitrate concentrations (mg/l)		Modified DRASTIC Classes	Covered area (Km^2)	Median values of Nitrate concentrations (mg/l)	
		Dry Season	Wet Season			Dry Season	Wet season
Very low	469.05	0.01	0.01	Very low	402.7	0.02	0.22
Low	621.94	10.5	17.5	Low	539.3	10	17
Medium	174.08	No data	No data	Medium	305.5	No data	No data
High	4.21	No data	No data	High	21.8	No data	No data

It is clear that no matter how infrequent or scarce lineament features are, they continue to play a significant part in opening up routes for contaminants to enter groundwater, increasing the extent and rate of penetration through fractures and joints. As shown in (Fig. 6), the conventional model assigns a light green colour to a tiny segment of the Makok anticline in the centre of the examined basin and classifies it as having low vulnerability.

The same region, however, is coloured orange in the lineament-modified model and categorised to be moderately vulnerable (Figure 7).

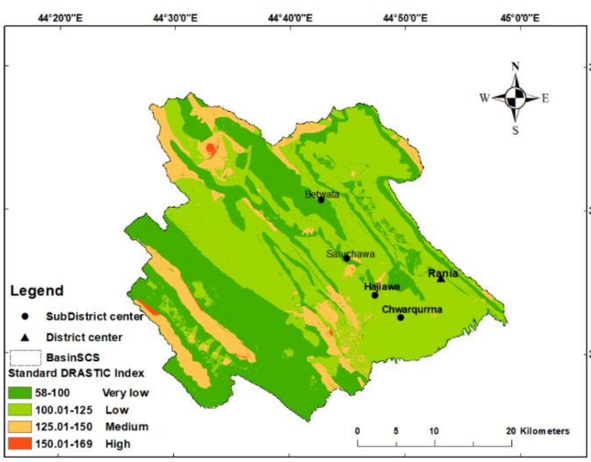

Figure 6: Generic DRASTIC map of the studied basin.

Obtained results of nitrate concentration display a noticeable variation over dry and wet seasons. The median values of the collected samples are only 10.5 mg/l in the dry season while going up, as high as 17.5 mg/l in the wet season. The increase is linked to natural sources, including various fertilisers and pesticides used by farmers that contain nitrogen, as well as the significant influence of precipitation in the penetration of nitrate.

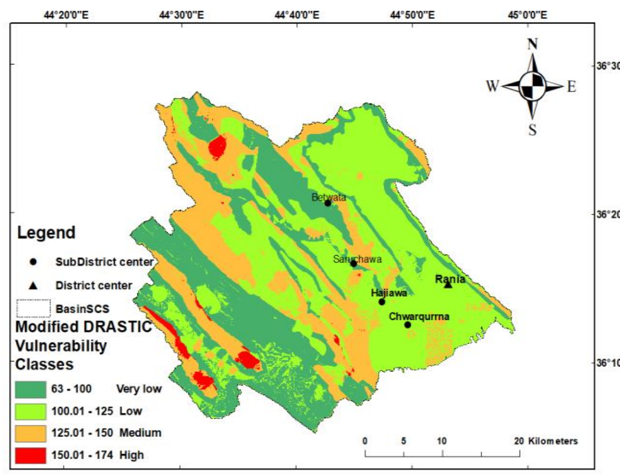

Figure 7: Modified - DRASTIC map of the studied basin.

Variations in the ranges of nitrate concentrations somehow mirrored the lineament-modified characterisation as shown in Table 4, making the case for incorporating the lineament index into the DRASTIC model more vital. Nitrate level recorded areas classed as very low vulnerability gave a median value of 0.22 mg/l, while it was as high as 17 mg/l in samples from low vulnerability areas.

3.3 Hazard maps

1. Unclassified hazard map

Numerous major hazard types (point, line, and polygon) have been identified in the studied basin as displayed in (Fig. 8). It is evident that most of the point hazards, such as car parking areas, open sports stadiums, and allotment gardens, are located in or very close to the district or sub-district centres in the studied basin. Polygon hazards such as urban areas with no sewer systems, graveyards, tourist spots, and intensively agricultural lands with a high demand for fertilizers and pesticides are mainly situated in rural undeveloped areas.

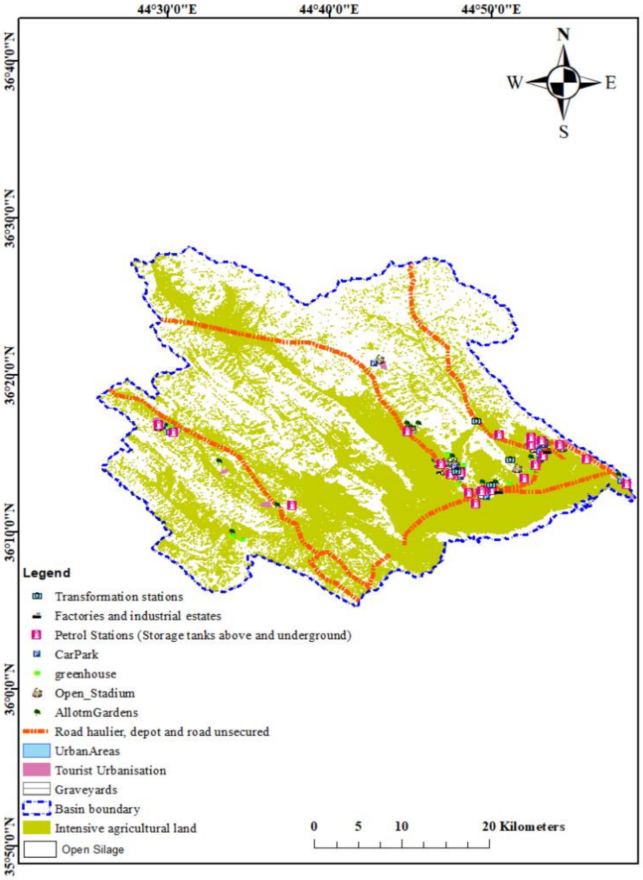

Figure 8: Map of the unclassified hazards in the studied basin.

Rania Plain, dominated by intensive agricultural activities, stands out in the southern parts of the basin. Linear hazards are represented by major paved roads and some unsecured roads leading up to the villages in the mountainous regions. There are considerable regional variations in the distribution of hazards, their size, and how damaging they are. The overall data display and the resolution of the hazard map, while still unclassified, become challenging in areas where multiple hazards overlap within nearby raster cells, leading to an increase in the corresponding harmfulness classes.

2. Classified hazard map

The classed map displays the hazards based on the hazard index class, which stands for the hazard level. The final map, depicted in (Fig. 9), was produced and categorized using the ranges suggested by [20]. It is obvious that 70.6 % is indexed as having no or a deficient level of hazard. The second largest share of the studied area (29.1 %) is indexed as low hazard. The moderate,

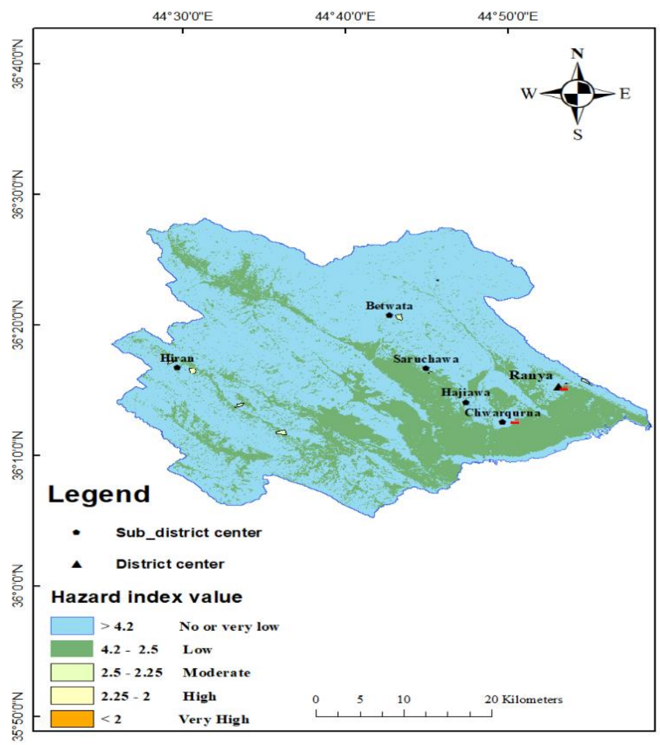

Figure 9: Classified hazard map of the studied basin.

Combining the vulnerability map with the classified hazard map is helpful to conduct risk assessments and subsequently prevent possible groundwater pollution [20].

3. Risk intensity index (RII) map

In this project, the risk intensity index and the risk intensity map were produced when the classified hazard map was combined with the lineament-modified map. The contamination risk map shows a spatial distribution different from those categorized by the intrinsic vulnerability index. In some areas where urbanization, industrial or agricultural activities are intense, the contamination risk ranges from moderate to very high. In comparison, the vulnerability index is found to be very low to low, although the majority of the study area is assigned to low and moderate risk level as shown in Table 6. As can be depicted from the risk intensity map in (Fig. 10), the risk classes within the studied basin change spatially and range from very high to very low as per the variety of hazard types that occur.

It is critically vital to remember though, that the functionality of a risk intensity map is quite different from vulnerability maps of groundwater. Risk maps are more time-specific and only represent the current situation and may very well expire or at least give a false assessment, unlike groundwater vulnerability maps that are more independent of their production time.

Table 6: Classification of the studied basin based on hazard Index, corresponding covered area and risk intensity index .

DRASTIC (Π) index	Hazard Index	Hazard Level	Area (Km2)	Area %	1/HI	Π.1/HI	Risk class	Risk level	Area (Km2)	Area %
>100	0 – 24	No or very low	897	70.66	>0.042	>4.2	1	Very low	72.97	5.6
100 – 125	25 – 48	Low	369.3	29.1	0.04-0.02	4.2-2.5	2	Low	651.9	51.5
125 - 150	49 – 65	Medium	1.83	0.14	0.02-0.015	2.5-2.25	3	Moderate	404.2	31.9
150 – 200	66 – 96	High	1.15	0.09	0.015-0.01	2.25-2	4	High	136.9	10.8
<200	96 - 120	Very high	0.02	0.001	0.01-0.008	<2	5	Very high	3.2	0.2

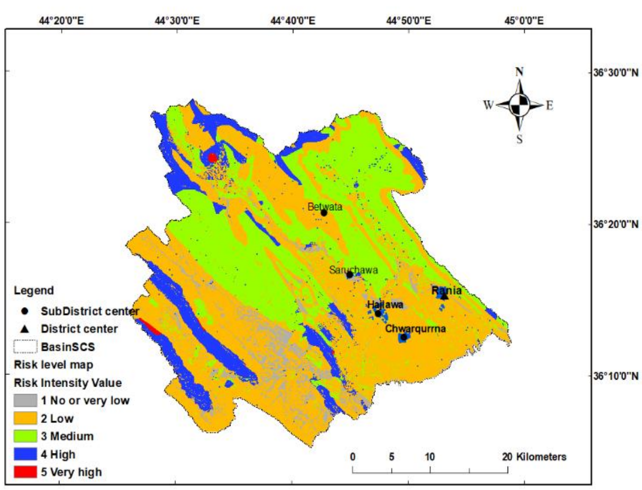

Figure 10: Risk intensity map of the studied basin.

This is because of the variable nature of the existing and potential hazards on the ground that can change widely and rapidly while the vulnerability maps are more related to the fixed natural hydrogeological settings of the basin and less dependent on short-term variations. This is why risk intensity maps, however complete and adequately combined, still need continuous updates and modifications.

Conclusions

Pollution has recently emerged as a significant obstacle to fully utilizing groundwater. Evaluation of the contamination risk in the basin of Rania was the prominent goal of this project.

The studied basin is divided into four vulnerability zones in terms of groundwater vulnerability based on the index values computed through the standard DRASTIC model. The four index value ranges and their corresponding vulnerability classes are very low (58 – 100), low (100 – 125), medium (125 – 150), and high (150 – 169), respectively.

Modification through adding the lineament index as an extra parameter to the original DRASTIC parameters was attempted to synchronise it with a more basin-specific feature. However, With the exception of minor variations in the areas encompassed by each vulnerability classification, no significant or definitive contrasts emerged in the intensity and categorisations presented by the two models.

The proposed categorization of the groundwater vulnerability in the studied basin is found to be a close-to-reality scenario since it was validated through comparison with nitrate level concentration in 60 water samples (in wet and dry seasons) collected from 17 wells and 13 springs in the studied basin.

Risk mapping of the studied basin offers a positive assessment of the groundwater. It indicates that (5.6%) of the studied basin is categorized as having a very low risk of groundwater contamination and (51.5%) which is the largest part categorized as having a low risk of contamination followed by (31.9 %) as moderate risk. The high and very high classes, however, take very smaller portions of (10.8 %), and (0.2 %) respectively.

Authors contribution

The project core framework was designed by [Ata Omer Ssalih], who also handled most of the material preparation, data gathering, and analysis. [Diary Ali Al-Manmi] assisted in data collection, literature review, and verification of some of the outcomes. [Ata Omer Ssalih] drafted the manuscript and the final version was read and approved by both authors.

Conflict of interests

The authors have no financial or proprietary interests in any material discussed in this article.

Acknowledgements

The authors would like to thank the Sulaimani Groundwater Directorate, Dokan Meteorological Station, and Rania Water Directorate, as they permitted the authors to utilise their archived well log and meteorological data in this research.

References

[1] Lee, S., Kim, Y.S. and Oh, H.J. Application of a weights-of-evidence method and GIS to regional groundwater productivity potential mapping. *Journal of Environmental Management*, **96**(1), pp.91-105. https://doi.org/10.1016/j.jenvman.2011.09.016 (2012)

[2] Arulbalaji, P., Padmalal, D., & Sreelash, K. GIS and AHP techniques-based delineation of groundwater potential zones: a case study from southern Western Ghats, India. *Scientific reports* **9**(1): 2082 (2019)

[3] Andualem, T. G, & Demeke, G. G. Groundwater potential assessment using GIS and remote sensing: A case study of Guna tana landscape, upper Blue Nile Basin, Ethiopia. *Journal of Hydrology: Regional Studies* **24**: 100610. (2019)

[4] Alikhanov, B, Juliev, M, Alikhanova, S, Mondal, I. Assessment of influencing factor method for delineation of groundwater potential zones with geospatial techniques. Case study of Bostanlik district, Uzbekistan. *Journal of Groundwater for Sustainable Development* **12**: 100548. https://doi.org/10.1016/j.gsd.2021.100548 (2021)

[5] Younis, J., Ahmed, C. Application of Remote Sensing and GIS to Mapping Groundwater Potential Zones of Khazir River Basin, Northern Iraq. Iraqi National Journal of Earth Science (INJES). 22. 10.33899/earth.2022.176650. (2022).

[6] Salih, A.O., & Al-Manmi, D.A. "Strategies for Sustainable Water Management: Hydrochemical Profiling and Protection Zone Design in Rania Basin, Iraq", *ARO-THE Scientific Journal of Koya University*, Vol. XII, No.2 (2024). pp. 107-118. doi: 10.14500/aro.11435

[7] Ali, A., Al-Abadi, A. Groundwater Vulnerability Evaluation in the Nineveh Plain, Northern Iraq, using a GIS-based DRASTIC Model. *Iraqi National Journal of Earth Science (INJES)*, 2021; 21(2): 78-92. doi: 10.33899/earth.2021.170392

[8]Ahmed, C., Younis, J. Evaluation of Groundwater Vulnerability to Pollution Using the DRASTIC Model and GIS in the Plain Part of the Khazir River Basin, Northern Iraq. *Iraqi National Journal of Earth Science (INJES)*, 23(2): 1-19. doi: 10.33899/earth.2023.138170.104 (2023).

[9] Morris, B. L., & Foster, S. D. Cryptosporidium contamination hazard assessment and risk management for British groundwater sources. *Water Science and Technology* **41**(7): 67-77. https://doi.org/10.2166/wst.2000.0117 (2000)

[10] Selvam, S., & Palanivelu, K. Lineament Modified DRASTIC Model for Groundwater Vulnerability Assessment in Ponnaiyar River Basin, South India Using Remote Sensing and GIS. *Hydrogeology Journal* **23**(4): 777-795 (2015)

[11] De Luca, D. A., Lasagna, M., Le Donne, E., & Sethi, R. Groundwater Vulnerability Assessment Combining DRASTIC with Geological Lineaments: The Mediterranean Coastal Aquifer of Monastir (Tunisia) as a Case Study. Hydrogeology Journal 25(2): 463-478 (2017)

[12] Mogaji, K. A., Dada, S. S., & Agboola, O. P. Application of Lineament-modified DRASTIC Method to Groundwater Vulnerability Mapping in Part of Southwestern Nigeria. *Arabian Journal of Geosciences* **11**(16): 1-11 (2018)

[13] Werz, H., & Hötzl, H. J.. Groundwater risk intensity mapping in semi-arid regions using optical remote sensing data as an additional tool. *Hydrogeology Journal* **15**(6): 1031-1049 (2007)

[14] Mimi, Z., & Assi, A. Intrinsic vulnerability, hazard, and risk mapping for karst aquifers: A case study. *Journal of Hydrology* **364**(3–4): 298–310. https://doi.org/10.1016/j.jhydrol.2008.11.008 (2009)

[15] Al-Manmi, D A M, Abdullah, T O, Al-Jaf, P M, & Al-Ansari, N. Soil and Groundwater Pollution Assessment and Delineation of Intensity Risk Map in Sulaymaniyah City, NE of Iraq.*Water*, **11**(10): 2158. http://dx.doi.org/10.3390/w11102158 (2019)

[16] Mohammed, S. A., Nejad, R. A., & Hamamin, D. F. Vulnerability pesticide DRASTIC and risk intensity map for multi aquifer units: A case study from Basara basin, Iraqi Kurdistan Region. *Eurasia Journal of Biosciences* **14**(2): 6119–6131 (2020)

[17] Jassim, S. Z., & Goff, J. C. Geology of Iraq (First edition). Published by Dolin, Prague and Moravian Museum, Brno, Czech Republic (2006)

[18] Salih, A.O., & Al-Manmi, D.A. DRASTIC model adjusted with lineament density to map groundwater vulnerability: a case study in Rania basin, Kurdistan, Iraq. *Environmental Science and Pollution Research* **28**: 59731–59744. https://doi.org/10.1007/s11356-021-14912-4 (2021)

[19] Sissakian, V. K. Geological Map of Arbeel and Mahabad Quadrangles, scale 1:250000. State Establishment of Geological Survey and Mining, Iraq-Baghdad (1997)

[20] Zwahlen, F. Vulnerability and risk mapping for the protection of carbonate (karst) aquifers, final report (COST action 620), European Commission, Directorate XII Science, Research and Development, Report EUR 20912, Brussels. Pp.297 (2003)

[21] Aller, L., Bennett, T., Lehr, J.H., Petty, R.H., & Hackett, G. DRASTIC: A Standardized System for Evaluating Groundwater Pollution Potential Using Hydrogeologic Setting. USEPA Report 600/2-87/035, Robert S. Kerr Environmental Research Laboratory (1987)

[22] Al-Rawabdeh, A.M., Al-Ansari, N.A., Al-Taani, A.A., Al-Khateeb, F.L., & Knutsson, S. Modeling the Risk of Groundwater Contamination Using Modified DRASTIC and GIS in Amman-Zerqa Basin, Jordan. *Open Engineering* **4**: 264-280. http://dx.doi.org/10.2478/s13531-013-0163-0 (2014)

[23] Lattman, H., & Parizek, R. Relationship between Fracture Traces and the Occurrence of Ground Water in Carbonate Rocks. Journal of Hydrology 2: 73-91. http://dx.doi.org/10.1016/0022-1694(64)90019-8 (1964)

[24] Secunda S., Collin M., & Melloul A. J. Groundwater Vulnerability Assessment Using a Composite Model Combining DRASTIC with Extensive Land Use in Israel's Sharon Region. *Journal of Environmental Management* **54**(1): 39-57. (1998)

[25] Abdullah, T.O. Evaluation of Groundwater Vulnerability to Pollution using three different assessment models in the Halabja-Saidsadiq Hydrogeological Basin, North-East/Iraq. Dissertation, University of Sulaimani (2018)

[26] Werz, H. The Use of Remote Sensing Imagery for Groundwater Risk Intensity Mapping in the Wadi Shueib, Jordan. Dissertation, University of Karlsruhe, Germany) (2006)

[27] Hötzl, H., Delporte, C, Liesch, T, Malik, P, Neukum, C, & Svasta, J. Risk Assessment Concept. In F. Zwahlen (Ed.), *COST Action 620-Vulnerability and Risk Mapping for the Protection of Carbonate (Karst) Aquifers Final Report*, **108-113**, Public European Communities, Luxembourg (2004).